

## Electronic supplementary information (ESI)

# Unusual composition dependence of magnetic relaxation for $\text{Co}^{\text{II}}_{1-x}\text{Ni}^{\text{II}}_x$ chain-based metal-organic frameworks

Yan-Qin Wang, Ai-Ling Cheng, Pei-Pei Liu, and En-Qing Gao

**Synthesis of 1:** A solution of HL (0.018 g, 0.10 mmol) and  $\text{NaN}_3$  (0.026 g, 0.40 mmol) in ethanol (3 ml) and water (5 ml) was added into the ethanol solution (2 ml) of  $\text{Co}(\text{NO}_3)_2 \cdot 6\text{H}_2\text{O}$  (0.058 g, 0.20 mmol). The mixture was stirred for a few minutes and then filtered. Slow evaporation of the clear pink filtrate at room temperature afforded pink crystals of **Co-1** after one day. Yield: 57% based on HL. Elem anal. Calcd (%) for  $\text{C}_8\text{H}_8\text{CoN}_4\text{O}_5$ : C, 32.12; H, 2.70; N, 18.73. Found: C, 32.34; H, 2.92; N, 18.56. IR ( $\text{cm}^{-1}$ , KBr):  $\nu(\text{N}_3)$  2069s,  $\nu(\text{COO})$  1618s and 1383s.

**Crystal data of 1:**  $\text{C}_8\text{H}_8\text{CoN}_4\text{O}_5$ ,  $M_r = 299.11$ , Orthorhombic, space group  $Pnma$ ,  $a = 7.604(3)$  Å,  $b = 7.312(3)$  Å,  $c = 18.317(7)$  Å,  $V = 1018.4(7)$  Å<sup>3</sup>,  $Z = 4$ ,  $\rho_{\text{calcd}} = 1.951$  g cm<sup>-3</sup>,  $T = 293$  K,  $\mu(\text{Mo K}\alpha) = 1.708$  mm<sup>-1</sup>,  $\lambda = 0.71073$  Å,  $2\theta_{\text{max}} = 55.06^\circ$ , 5850 reflections measured, 1252 unique,  $R_{\text{int}} = 0.0523$ ,  $R_1[\text{I} > 2\sigma(\text{I})] = 0.0551$ ,  $wR_2(\text{all data}) = 0.1750$ ,  $S = 0.956$ . Intensity data were recorded on a Bruker Apex II CCD system with Mo- $K\alpha$  Radiation. Empirical absorption corrections were applied (G. M. Sheldrick, *SADABS, Program for Empirical Absorption Correction*; University of Göttingen: Göttingen, Germany, 1996). The structure was solved by direct methods and refined by full-matrix least-squares techniques on  $F^2$  using SHELXTL (G. M. Sheldrick, *SHELXTL*; Bruker Analytical X-ray Instruments Inc.: Madison, Wisconsin, USA, 1998). All non-hydrogen atoms were treated with anisotropic displacement parameters for all non-hydrogen atoms. The hydrogen atoms attached to carbon atoms were placed in calculated positions and refined using the riding model. The hydrogen atoms of the free water molecule (O3) were located from the difference Fourier map, and to obtain reasonable geometric parameters for the molecule, three restraints on the O-H and H...H distances were used.

**General synthetic procedure for the  $\text{Co}^{\text{II}}_{1-x}\text{Ni}^{\text{II}}_x$  compounds:** A water solution (2 ml) of HL (0.072 g, 0.40 mmol) was mixed with the methanol solution (4 ml) containing  $\text{Co}(\text{NO}_3)_2 \cdot 6\text{H}_2\text{O}$  and/or  $\text{Ni}(\text{NO}_3)_2 \cdot 6\text{H}_2\text{O}$  (the total quantity of the metal salts is 0.40 mmol), then  $\text{NaN}_3$  (0.10 g, 1.6 mmol) was added, yielding polycrystalline precipitates. After refluxing for 3 hours, the solids were collected by filtration, washed by water and methanol, and dried in air. Yields 40-60%. The compounds with  $x = 0, 0.11, 0.21, 0.31, 0.45, 0.65, 0.79,$  and 1 were obtained from the reactions with  $x_{\text{synthesis}} = 0, 0.10, 0.20, 0.30, 0.50, 0.65, 0.80,$  and 1 respectively. The metal ratios in the products were determined by the inductively coupled plasma (ICP) atomic emission spectrometry. The colour of the compounds changes gradually from pink to green as  $x$  increases from 0 to 1. The CHN elemental analytic data of these compounds are very similar owing to the similarity of Co and Ni in atomic weight. They exhibit almost identical IR spectra and very similar X-ray diffraction patterns (Fig. S1).

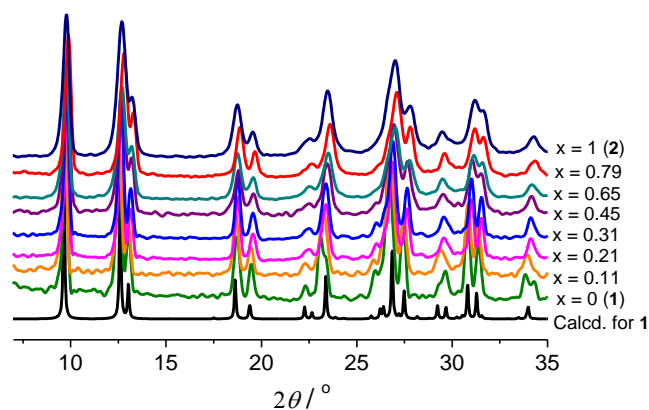


**Fig. S1.** Powder X-ray diffraction patterns of the  $\text{Co}^{\text{II}}_{1-x}\text{Ni}^{\text{II}}_x$  compounds

**Structure Determination of 2 by Powder X-Ray Analysis.** Our efforts to grow crystals of **2** suitable for single-crystal X-ray crystallography turned out in vain. Since powder X-ray diffraction measurements indicated that **1** and **2** are isomorphous, the structure of **2** was determined from the powder diffraction using the Reflex and DMol<sup>3</sup> programs implemented in the Materials Studio software,<sup>1</sup> with the structure of **1** as the starting model. Firstly, the unit cell was refined by the Pawley method<sup>2</sup> provided in Reflex. The final Pawley refinement including the pseudo-Voigt peak shape profile parameters, the 20-term background polynomials, the Rietveld asymmetry correction parameters and the Bragg-Brentano zero-point shift parameter gave a satisfactory  $R_{\text{wp}}$  value of 5.81%. The calculated and experimental powder patterns are compared in Fig. S2. Secondly, the atomic coordinates within the fixed unit cell determined by the Pawley refinement were optimized by DFT (density functional theory) lattice energy calculations using the DMol<sup>3</sup> module<sup>3</sup> (BP functional, DND basis set, and effective core potentials for metals, with coarse convergence criteria).

The optimized structure was used as input for Rietveld refinements<sup>4</sup> with Reflex. Because of the limited data of powder diffraction, the independent refinements of individual atomic coordinates led to chemically insensible results. Therefore, rigid-body Rietveld refinements were applied, in which the organic ligand, the azide ligand, and the lattice water molecule were defined as independent motion groups, which can translate and rotate with fixed bond distances and angles within each group. A global isotropic temperature factor was applied and refined, because the refinement of independent atomic temperature factors with the limited powder diffraction data is unreliable. The following parameters were also adjusted in the refinements: the pseudo-Voigt peak shape profile parameters, the Bragg-Brentano zero-point shift parameter, the 20-term polynomial background parameters, the Rietveld asymmetry correction parameters, and the March–Dollase parameters for the effects of preferred orientation. The final refinements led to a  $R_{\text{wp}}$  value of 6.67% with reasonable structure parameters.

A summary of the refinement data is given in Table S1. The diagram comparing the calculated and experimental powder patterns is shown in Fig. S3. The atomic coordinates and selected bond parameters are given in Tables S2 and S3, respectively..

#### References

- 1 *Materials Studio 6.1*. Accelrys Software Inc.: San Diego, CA, 2009.
- 2 G. S. Pawley, *J. Appl. Crystallogr.* **1981**, *14*, 357.
- 3 B. J. Delley, *Chem. Phys.* **1990**, *92*, 508; B. J. Delley, *Chem. Phys.* **2000**, *113*, 7756.
- 4 H. M. Rietveld, *J. Appl. Crystallogr.* **1969**, *2*, 65; R. A. Young, *The Rietveld Method*, IUCr Monographies of Crystallography 5, Oxford University Press: Oxford, 1993.

**Table S1.** Crystal Data and Structure Refinement for Compound **2**

Formula	$C_8H_8N_4NiO_5$	$M_r$	298.86
Crystal system	Orthorhombic	space group	$Pnma$
$a$ [Å]	7.6031(6)	$b$ [Å]	7.2312(6)
$c$ [Å]	18.195(2)	$V$ (Å <sup>3</sup> )	1000.4(2)
$Z$	4	$\rho_{\text{calcd}}$ [g cm <sup>-3</sup> ]	1.984
$T$ [K]	295	$2\theta$ range [°].	5.0-60.0
$R_{\text{wp}}$	0.0667	$R_p$	0.0510

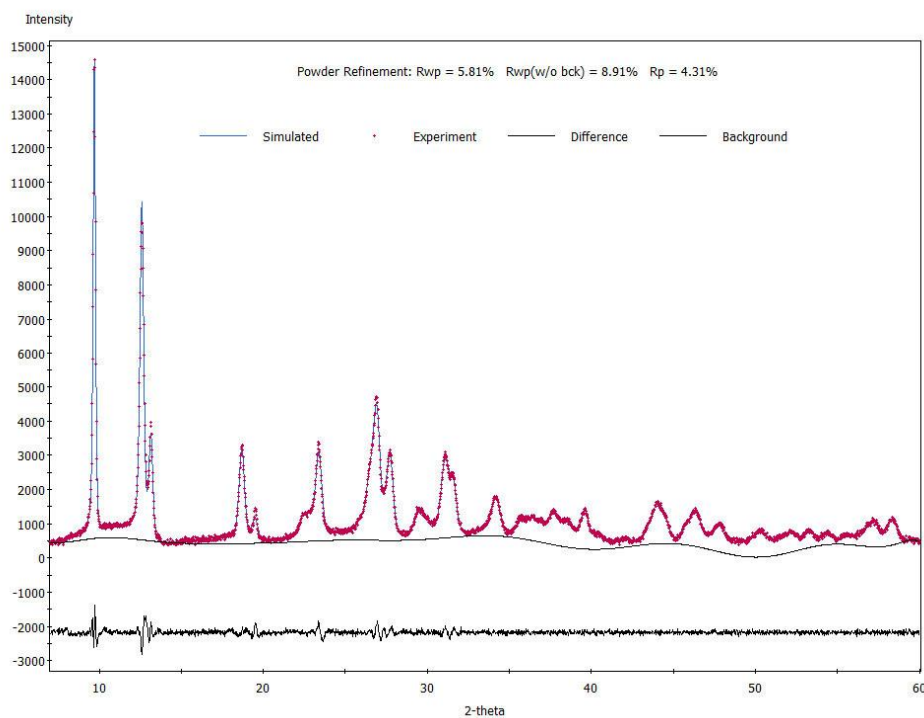


**Fig. S2.** Comparison of the calculated and experimental powder patterns for the final Pawley refinement.

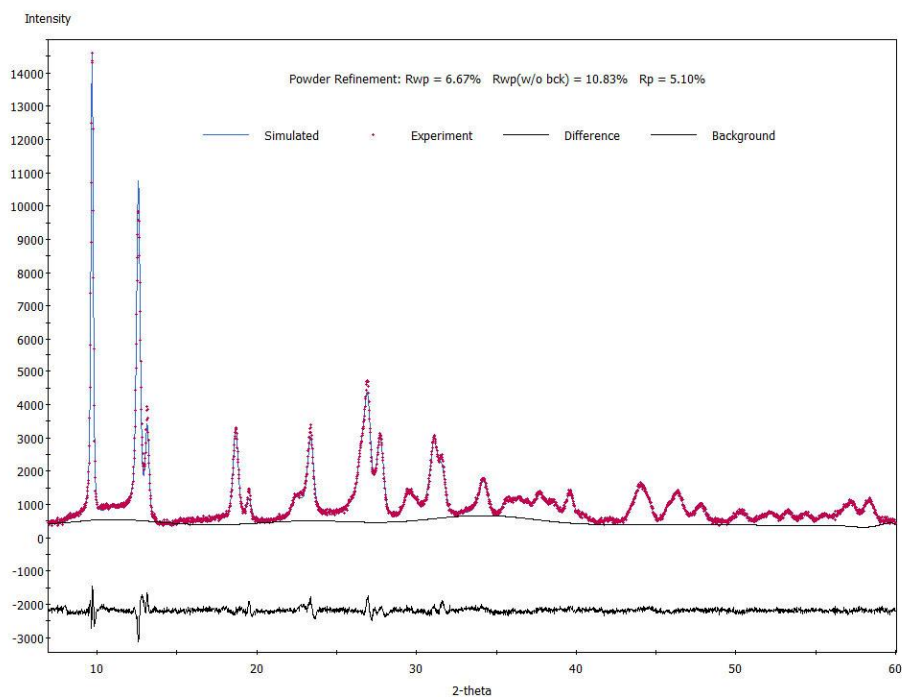


**Fig. S3.** Comparison of the calculated and experimental powder patterns for the final Rietveld refinement.

**Table S1** Atomic coordinates of **2** in the final rigid-body Rietveld refinement

Atom	Wyckoff position	Site symmetry	x/a	y/b	z/c
Ni1	4a	-1	1/2	0	1/2
N1	4c	.m.	0.5886(9)	1/4	0.4577(5)
N2	4c	.m.	0.6691(9)	1/4	0.4013(5)
N3	4c	.m.	0.7431(9)	1/4	0.3461(5)
N4	4c	.m.	0.4896(6)	1/4	0.8749(7)
O1	8d	1	0.5336(6)	0.09142	0.6102(3)
O2	8d	1	0.7452(6)	0.09160	0.9907(3)
C1	4c	.m.	0.5267(6)	1/4	0.6403(3)
C2	4c	.m.	0.5152(6)	1/4	0.7225(3)
C3	8d	1	0.5091(6)	0.08434	0.7616(3)
H3A	8d	1	0.5093(6)	-0.04725	0.7340(3)
C4	8d	1	0.4970(6)	0.08686	0.8380(3)
H4A	8d	1	0.4851(6)	-0.03800	0.8704(3)
C5	4c	.m.	0.4851(6)	1/4	0.9556(3)
H5A	8d	1	0.4162(6)	0.37390	0.9742(3)
C6	4c	.m.	0.6779(6)	1/4	0.9827(3)
O3	4c	.m.	0.2908(14)	-1/4	0.8437(7)
H3WA	4c	.m.	0.2402(14)	-1/4	0.7944(7)
H3WB	4c	.m.	0.1924(14)	-1/4	0.8784(7)

**Table S2** Bond distances (Å) and angles (deg) of **2**.

Ni1–O1	2.127(5)	Ni1–O2C	2.054(4)
Ni1–N1	2.077(4)	C1–O1	1.272(3)
C1–C2	1.498(8)	C6–O2	1.263(3)
C2–C3	1.394(4)	C5–C6	1.547(7)
C3–C4	1.393(8)	N4–C4	1.358(7)
N4–C5	1.469(14)	N1–N2	1.195(12)
N2–N3	1.151(12)		
O1–Ni1–O1A	180	N1–Ni1–N1D	180
O1–Ni1–N1D	87.716(3)	N1D–Ni1–O2C	93.195(3)
O1–Ni1–N1	92.284(4)	N1–Ni1–O2B	86.805(3)
O1–Ni1–O2B	93.704(4)	O2C–Ni1–O2B	180
O1–Ni1–O2C	86.296(4)	N2–N1–Ni1	118.971(4)
C1–O1–Ni1	132.945(4)	C6–O2–Ni1E	133.156(4)
O1–C1–O1G	128.738(3)	O2–C6–O2G	130.175(3)
O1–C1–C2	115.612(6)	O2–C6–C5	114.883(6)
C3–C2–C3G	118.483(3)	C3–C2–C1	120.758(6)
C4–C3–C2	120.009(6)	N3–N2–N1	178.4 (10)
N4–C4–C3	120.476(6)	N4–C5–C6	107.3(4)
C4–N4–C4G	120.537(3)	C4–N4–C5	119.672(6)
Ni1–N1–Ni1F	121.000(2)		

Symmetry codes: A = -x+1, -y, -z+1; B = -x+3/2, -y, z-1/2; C = x-1/2, y, -z+3/2; D = -x+1, y+1/2, -z+1;

E = 1.5-x, -y, 0.5+z; F = 1-x, 0.5+y, 1-z; G = x, 0.5-y, z

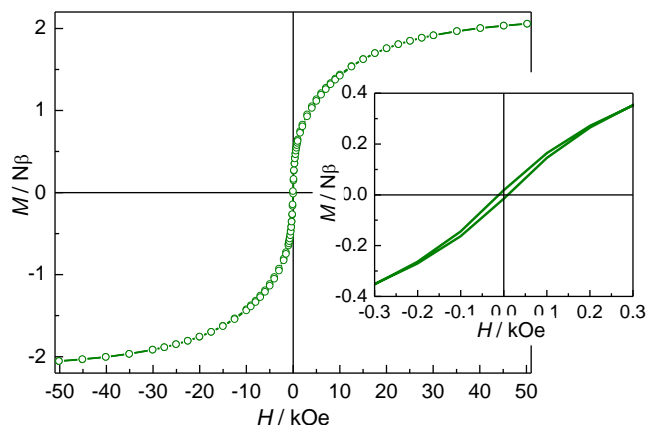


**Fig. S4** The field dependence of magnetization of **2** at 2 K. The inset shows the hysteresis loop at low-field.

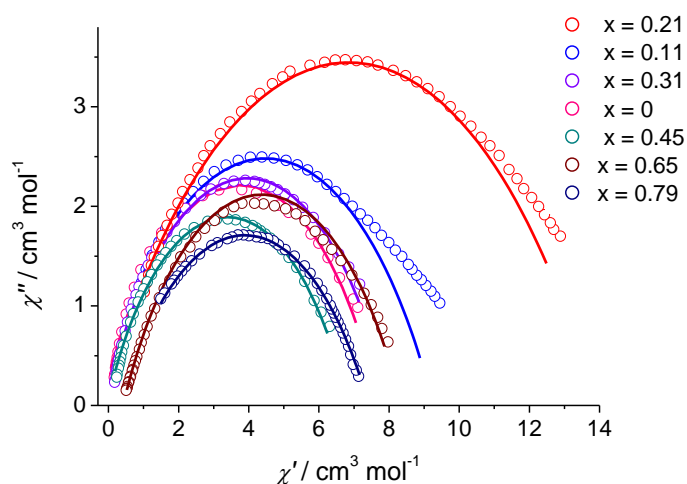


**Fig. S5** Cole-Cole diagrams for the  $\text{Co}^{\text{II}}_{1-x}\text{Ni}^{\text{II}}_x$  materials in the frequency range 1-1488 Hz with  $H_{\text{dc}} = 0$ ,  $H_{\text{ac}} = 3$  Oe. The solid lines represent the least-squares fitting with a generalized Debye model,  $\chi = \chi_s + (\chi_T - \chi_s) / [1 + (i\omega\tau)^{1-\alpha}]$ . Note that some Cole-Cole plots deviate from the Debye model fitting at the low-frequency ends (the right ends). This may indicate the existence of another relaxation, which is however not well separated from the main relaxation. Another possibility is that the general Debye model is just an approximation to the real relaxation process, not a universal model. The phenomena are open to further study.

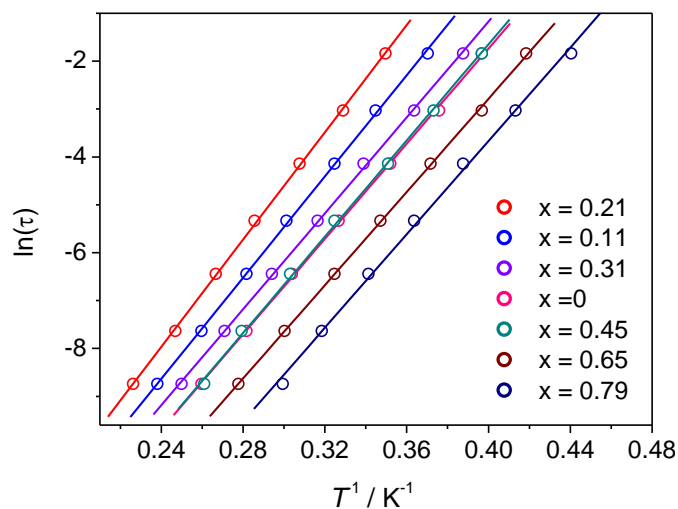


**Fig. S6** The Arrhenius-law fits for the  $\text{Co}^{\text{II}}_{1-x}\text{Ni}^{\text{II}}_x$  materials.

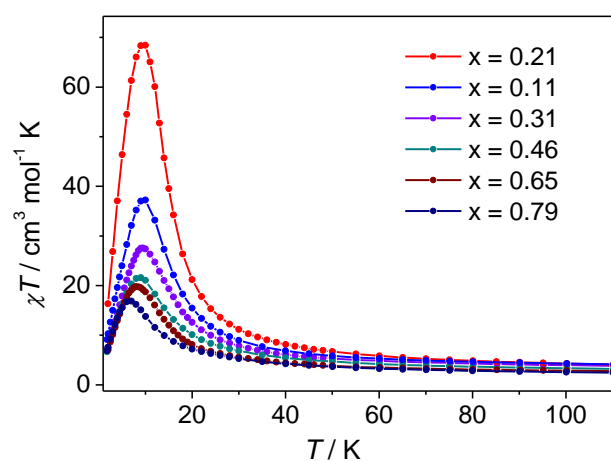


**Fig. S7** The  $\chi T$ - $T$  plots in the low-temperature region for the mixed-metal materials.

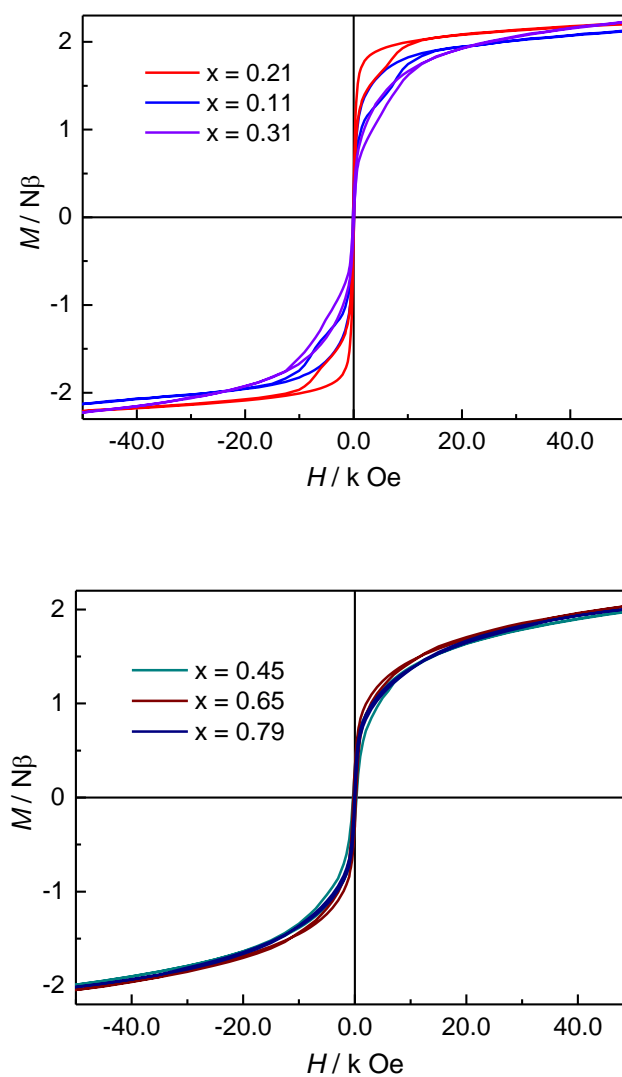


**Fig. S8** Hysteresis loops for the mixed-metal materials at 2 K.

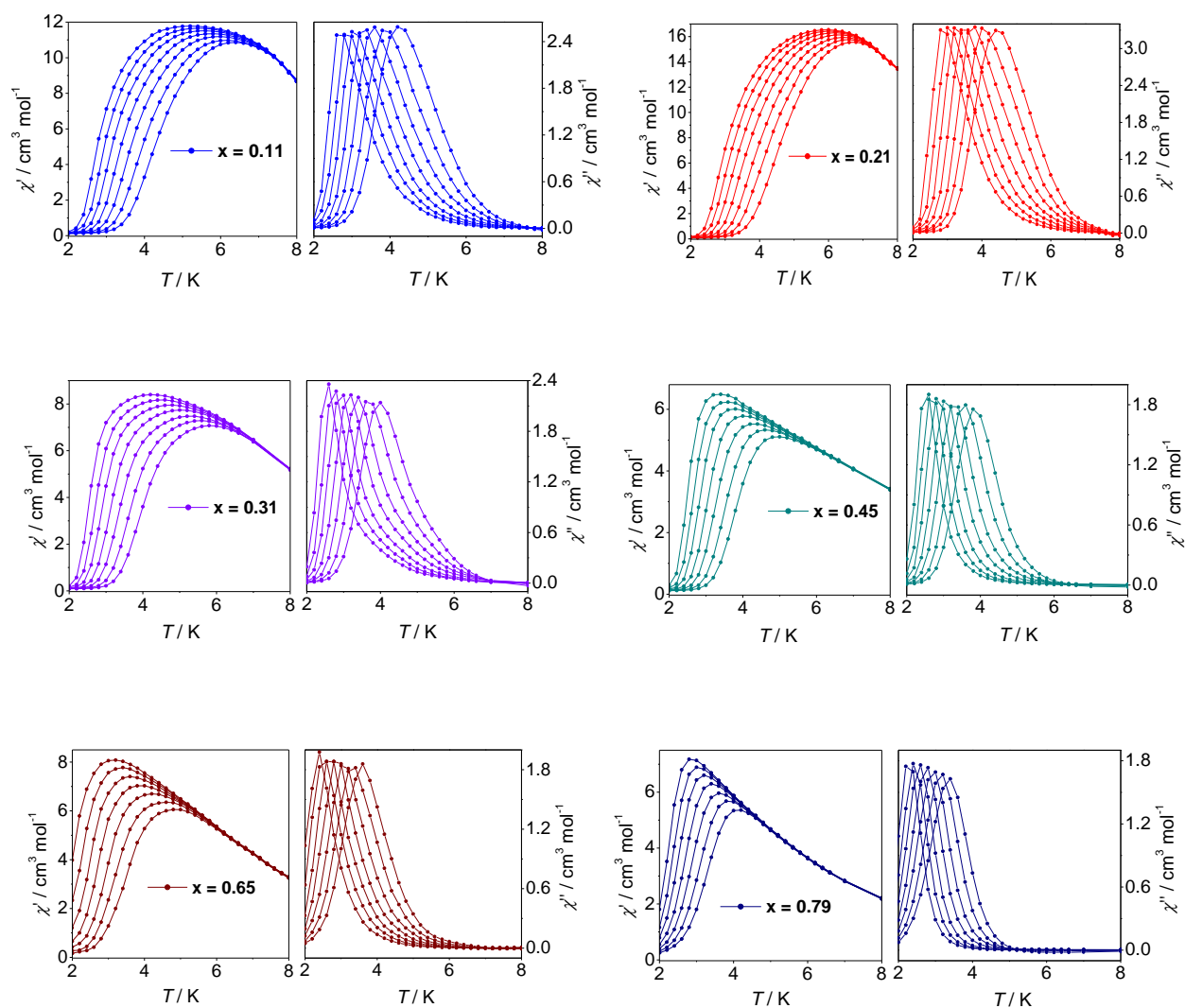


**Fig. S9**  $\chi'(T)$  and  $\chi''(T)$  plots for the mixed-metal materials at frequencies 1, 3.3, 10, 33, 100, 330 and 1000 Hz (from left to right) with  $H_{dc} = 0$  and  $H_{ac} = 3$  Oe.